Kinetics and Catalysis, Vol. 44, No. 1, 2003, pp. 40–53. Translated from Kinetika i Kataliz, Vol. 44, No. 1, 2003, pp. 47–61.

The Role of Singlet and Triplet Dioxygen Molecules in the EPR and ^{1}H NMR Spectrum Line Broadening

A. E. Gekhman*, N. I. Moiseeva, V. V. Minin*, G. M. Larin*, Yu. V. Kovalev***, Yu. A. Ustynyuk***, V. A. Rosniatovskii***, E. N. Timokhina****, K. V. Bozhenko****, and I. I. Moiseev***

** Kurnakov Institute of General and Inorganic Chemistry, Russian Academy of Sciences, Moscow, 117907 Russia*

*** Semenov Institute of Chemical Physics, Russian Academy of Sciences, Moscow, 117977 Russia*

**** Department of Chemistry, Moscow State University, Moscow, 119899 Russia*

***** Emanuel Institute of Biochemical Physics, Russian Academy of Sciences, Moscow, 117977 Russia*

Received April 22, 2002

Abstract—In the $Mo^{(VI)}/H_2O_2/H_2O$ system, the relaxation time (T_1) of protons in a water molecule and in a CH_3 group decreases 10 to 30 times under conditions of dismutation of H_2O_2 with the formation of $^1O_2(^1\Delta_g)$. It is experimentally found that the overequilibrium concentration of triplet dioxygen cannot be the reason behind a decrease in T_1 in the ^{1}H NMR spectra. Neither can it explain the anomalous line broadening in ESR spectra under conditions of $^1O_2(^1\Delta_g)$ formation in the systems $V^{(V)}/H_2O_2/AcOH$ and $Mo^{(VI)}/H_2O_2/H_2O$. *Ab initio* calculations showed that it is principle possible that the $^3O_4(^3\Sigma_g^- \cdot {}^1\Delta_g)$ molecule exists in a snake-like form and is formed by the reaction between $^3O_2(^3\Sigma_g^-)$ and $^1O_2(^1\Delta_g)$, which is the product of H_2O_2 decomposition in the systems $V^{(V)}/H_2O_2/AcOH$ and $Mo^{(IV)}/H_2O_2/H_2O$. The interaction of $^1O_2$ with the $^{\bullet}$OOH radical is exothermic (ΔQ = 2.30 kcal/mol) and leads to the formation of $^{\bullet}$OOOOH. It is assumed that the paramagnetic species of type $^{\bullet}$OOOOH or $^3O_4(^3A_1)$ that is formed in the reaction might be responsible for the spectral effects observed.

INTRODUCTION

Singlet dioxygen $^1O_2(^1\Delta_g)$ is known as an active oxidant in chemical and biological systems [1, 2]. It was found early in the 20th century that eosin, acridone, and some other dyes possess bactericide properties in light in the presence of oxygen [3, 4]. This phenomenon was called "photodynamic action" and was used in curing skin deceases. From the late 1970s and early 1980s, the photodynamic therapy of cancer (PTC) has been actively developed [5]. The photosensitized appearance of $^1O_2$ in a cell leads to cell degradation and thus forms the basis for PTC. Singlet dioxygen is capable of biologically oxidizing important molecules, such as unsaturated fatty acids, lipids, cholesterol, mono- and polysaccharides, amino acids and peptides, carotinoids, etc.

The reactions of $^1O_2(^1\Delta_g)$ with various chemical compounds are characterized by molecular rather than radical pathways. Thus, reactions with olefins, polyunsaturated, and aromatic compounds lead to the formation of dioxetenes and endoperoxides, which are the products of $^1O_2$ cycloaddition to the double bonds of unsaturated substrates, as well as hydroperoxides [6]. The formation of endoperoxides in the interaction with 9,10-dimethyl- or 9,10-diphenylanthracene is a probe reaction for the presence of $^1O_2(^1\Delta_g)$ [1]. Sulfide photooxidation [6, 7] with the formation of sulfoxides and sulfones occurs via the intermediate formation of a bipolar persulfoxide (**A**) or thiodioxirane (**B**) depending on the polarity of the solvent:

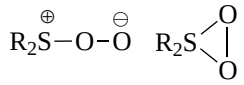

A **B**

The interaction of $^1O_2(^1\Delta_g)$ with thiols is assumed to form the basis for skin protection from the action of light [8].

At the same time, some reactions of $^1O_2(^1\Delta_g)$ are known to produce free radicals. Thus, stable nitroxyl radicals have been obtained by tertiary amine photooxidation [9].

There are no published data on the chemical interaction of $^1O_2(^1\Delta_g)$ with radicals, but it is known that peroxy radicals are efficient physical quenchers of $^1O_2$. Thus, acylperoxy radicals $CH_3COOO^{\bullet}$, $PhCOOOO^{\bullet}$, and p-$CH_3C_6H_4COOOO^{\bullet}$ quench $^1O_2$ luminescence in benzene with a rate constant of ~10^{10} mol l^{-1} s^{-1}, which is close to the diffusion limit [10]. The rate constant for

0023-1584/03/4401-0040$25.00 © 2003 MAIK "Nauka / Interperiodica"

quenching by the peroxy radicals $PhOO^{\bullet}$, *tert*-$BuOO^{\bullet}$, $PhCH_2OO^{\bullet}$, $Ph_2CHOO^{\bullet}$, and $Ph_3COO^{\bullet}$ in benzene is $(2–7) \times 10^9$ mol l^{-1} s^{-1} [11], which is close to the value of the rate constant of $^1O_2$ quenching by the superoxide radical ion in dimethyl sulfoxide (1.6×10^9 mol l^{-1} s^{-1} [12]). Stable nitroxyl radicals also quench $^1O_2$, but the rates of this process are lower ($10^5–10^6$ mol l^{-1} s^{-1} for aliphatic radials and $10^6–10^7$ mol l^{-1} s^{-1} for aromatic radicals [13]).

In the catalytic decomposition of H_2O_2 with the formation of singlet dioxygen in aqueous and acetic acid solutions, an unusual line broadening in the EPR spectra of various free radicals has been observed [14–18]. The rate constants of interaction of these radicals with $^1O_2$ differ by two or three orders of magnitude, whereas line broadening was comparable in all cases (7–10 G). In this paper, we analyze possible reasons for the phenomenon observed in the catalytic systems $H_2O_2/V^{(V)}$/AcOH and $H_2O_2/Mo^{(VI)}/H_2O$.

EXPERIMENTAL

Reagents and Materials

A phosphate buffer (pH 10.3) was prepared using a pH-150M pH meter (Belarus) and distilled water, H_3PO_4, and $Na_3PO_4 \cdot 12H_2O$ (analytical purity grade). In the experiments on the measurements of relaxation time (T_1) in the preparation of the buffer, D_2O was used. Acetic acid, CH_3COONa, and an aqueous solution of hydrogen peroxide (9.67 mol/l) were used without additional purification (all chemical purity grade). A concentrated solution of H_2O_2 (15 mol/l) was obtained by the distillation of commercial H_2O_2 (analytical purity grade). Stable nitroxyl radicals 1-H,2,5-dihydro-4-isopropyl-2,2,5,5-tetramethyl-imidasoline-N-1-oxyl (**1**) and 1-H,2,5-dihydro-3-carbamido-2,2,5,5-tetramethyl-pyrroline-*N*-1-oxyl (**2**) (all 95% pure according to GLC analysis), $(CH_3)_3CCOONa$, Na_2MoO_4, and NH_4VO_3 were used without additional purification. The $VO(acac)_2$ compound was recrystallized from $CHCl_3$.

Preparation of the Catalyst Solution

For the preparation of a solution of vanadium(V) in AcOH, 100 mg of finely dispersed NH_4VO_3 was boiled in 100 ml of AcOH for 4–5 h. Undissolved NH_4VO_3 was filtered off. The concentration of vanadium(V) in the resulting solution determined using an ICP–MS HP 4500 spectrophotometer (with an external standard NH_4VO_3) was 3.7×10^{-3} mol/l. In some kinetic experiments, $VO(acac)_2$, whose solubility in AcOH is much higher, was used as a catalyst precursor. EPR data showed that the vanadium(IV) signal from $VO(acac)_2$ disappears as soon as the first drops of H_2O_2 are added to the reaction solution. The replacement of $VO(acac)_2$ by NH_4VO_3 affects neither the composition of products of the reaction nor its rate.

H_2O_2 Decomposition

The reaction was carried out at 30°C in a thermostated Pyrex reactor equipped with a reflux condenser and a magnetic stirrer. In a typical run, 4.4 ml (42.5 mmol) of aqueous H_2O_2 (9.67 mol/l) was added to 1.33 mg (0.005 mmol) $VO(acac)_2$ in 50 ml AcOH. 2-Ethylanthracene (2-EA), CH_3COONa, $(CH_3)_3COONa$ and free nitroxyl radicals were dissolved in a reaction mixture before adding H_2O_2. Samples of the reaction mixture were diluted with a 3 ml 2 N aqueous solution of H_2SO_4. The rate of H_2O_2 decomposition was controlled by iodometric titration.

Measurement of O_2 Concentration Formed in H_2O_2 Decomposition

The concentration of oxygen in the solutions was determined by the amperometric method at a constant cathode potential using a Clarke-like measuring cell. The current passing through the measuring cell was proportional to the concentration of oxygen. The proportionality coefficient depended on the construction of the cell, medium pH, temperature, and stirring intensity near the electrode. The instrument was calibrated using a buffer solution saturated with air and oxygen [19]. In a typical run, a stirred cell for the determination of dioxygen concentration thermostated at 25°C was charged with a 1-ml solution of the phosphate buffer (pH 10.5) and 3 μl (0.05 mmol) of hydrogen peroxide (17 mol/l) was added. After thermostating, 1 μl Na_2MoO_4 in a phosphate buffer (10^{-2} mol/l) was added. In these runs, the initial concentration of H_2O_2 was chosen to be 0.05 rather than 0.2 mol/l as in the case of ESR spectra. This made it possible to increase the accuracy of the measurement of the maximum on the curve of the concentration of dissolved dioxygen. A tenfold decrease in the catalyst concentration (to 10^{-3} mol/l) led to a decrease in the rate of O_2 formation and an increase in the probability of its retaining in the liquid phase.

Spectral Studies

EPR spectra were recorded on a Radiopan SE/X-2542 instrument (9450 MHz, 0.5 G modulation amplitude) at 255–293 K. The internal field standard was 1,1-diphenyl-2-picrylhydrazyl (DPPG). Computational processing and the simulation of spectra were carried out according to the procedure described in [20]. The integral intensity of the signal was determined with reference to the third and fourth components of the signal of Mn/MgO, which was taken as an internal standard.

In a typical run, 1 ml (9.7 mmol) of the aqueous solution (9.67 mol/l) of H_2O_2 was added to 9 ml of glacial AcOH containing 10^{-2} mol/l $VO(acac)_2$. The resulting solution was placed into a flat EPR spectrometer cell (1 × 10 mm) equipped with two glass capillaries with a diameter of 0.2–0.3 mm. The capillaries were attached to the chambers filled with O_2, Ar, or CO_2. The

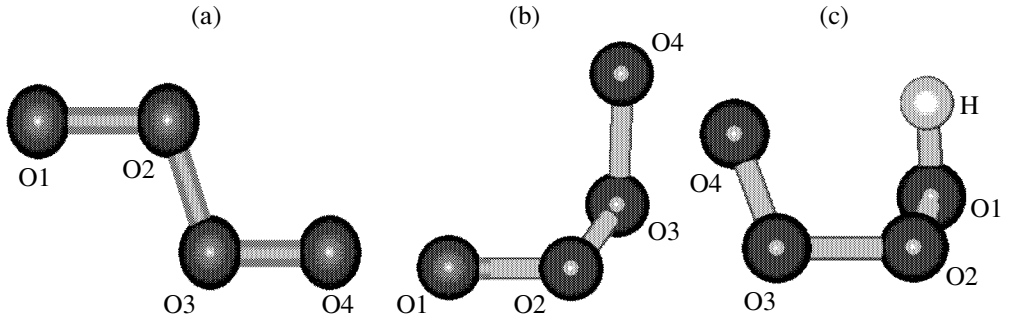

Fig. 1. The O_4 molecule in the (a) *trans* and (b) *twist* conformations and (c) radical $HO_4^{\bullet}$.

corresponding gas passed through a cell during spectrum recording.

The NMR spectra were recorded on a Bruker EPX-300 instrument. The values of T_1 were calculated using a computer program installed on a spectrometer computer. This program took into account the error of iteration convergence accurate to the second decimal digit. In a typical run, 0.037 ml (0.629 mmol) of the aqueous solution (8.5 mol/l) of H_2O_2 was added to 2.3 ml of the buffer solution (D_2O, pH 10.5) containing 10^{-2} mol/l Na_2MoO_4, 3×10^{-2} mol/l $(CH_3)_3CCOONa$, and 9×10^{-2} mol/l CH_3COONa. The resulting solution was placed into an ampule of the NMR spectrometer with an inner diameter of 5 mm.

The measurements of IR chemiluminescence of singlet dioxygen were carried out using a photometric setup ([21–23] and references therein) modified to register chemiluminescence. The sample radiation was focused on the entrance slit of an MDR-2 monochromator and then registered by an FEU-83 photomultiplier cooled to –60°C with liquid nitrogen vapors or measured by the same photomultiplier without a monochromator through a boundary light filter that transmits light in the region of $\lambda \geq 1000$ nm. The photomultiplier signal was amplified with a time constant of ~0.25 s and passed to a two-coordinate plotter or was registered by a computer. The setup made it possible to register spectra and the kinetics of damping luminescence in the range 400–1300 nm. The solution studied was inside a thermostated spectrophotometer cell with a thickness of 1 cm.

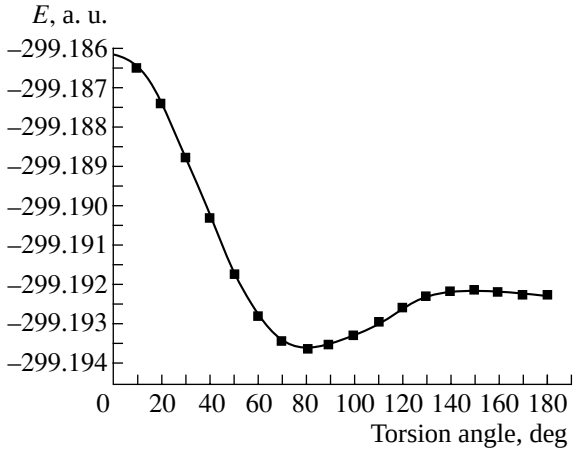

Fig. 2. Potential energy curve of the $O_4(^3\Sigma_g^- \cdot {}^1\Delta_g)$ molecule in the transition from *trans* to *cis* configuration depending on the torsion angle O4–O3–O2–O1 calculated in the UHF/6-311+G(d,p) approximation.

In a typical run, 0.18 ml (3.06 mmol) of the aqueous solution (17 mol/l) of H_2O_2 was added to 3 ml of glacial AcOH containing 10^{-2} mol/l $VO(acac)_2$. The resulting solution was placed in a glass cell (1×3 cm). The kinetics of chemiluminescence was studied at 22°C. The GraFit program package was used for mathematical processing.

Quantum Chemical Calculations

Ab initio calculations of the triplet $^3O_4(^3\Sigma_g^- \cdot {}^1\Delta_g)$ molecule were carried out. This molecule is expected to form via the reaction of $^3O_2(^3\Sigma_g^-)$ with $^1O_2(^1\Delta_g)$:

$$^3O_2(^3\Sigma_g^-) + {}^1O_2(^1\Delta_g) \rightleftharpoons {}^3O_4(^3\Sigma_g^- \cdot {}^1\Delta_g). \qquad \text{(I)}$$

We considered *trans* ($^3B_{3g}$, Fig. 1a), nonplanar spiral *twist* ($^3A_1$, Fig. 1b), and *cis* ($^3B_1$) conformations of the $^3O_4(^3\Sigma_g^- \cdot {}^1\Delta_g)$ molecule. To determine the ground-state geometry and the conformational stability of this molecule, we calculated the potential energy curve (PEC) of rotation around the central O–O bond (Fig. 2) in the framework of the unrestricted Hartree–Fock (UHF) method using the standard valence-split 6-311+G(d,p) basis set. The curve corresponding to the minimal energy path for the transition of the $^3O_4(^3\Sigma_g^- \cdot {}^1\Delta_g)$ molecule from the *twist* conformation to *trans* and *cis* conformations was calculated with the step Δ(O4O3O2O1) = 10°. According to our calculations, *twist* and *trans* con-

formation of the $^3O_4(^3\Sigma_g^- \cdot {}^1\Delta_g)$ molecule are more energetically favorable.

Reaction (I) is equilibrium. The forward reaction leads to the formation of the $^3O_4(^3\Sigma_g^- \cdot {}^1\Delta_g)$ molecule, and the reverse reaction leads to the dissociation of $^3O_4(^3\Sigma_g^- \cdot {}^1\Delta_g)$ into $^3O_2(^3\Sigma_g^-)$ and $^1O_2(^1\Delta_g)$. To study the stability of $^3O_4(^3\Sigma_g^- \cdot {}^1\Delta_g)$, we calculated PEC corresponding to the dissociation of *twist* and *trans* conformations of the $^3O_4(^3\Sigma_g^- \cdot {}^1\Delta_g)$ molecule. Both PECs were calculated for the R(O2–O3) distance in $^3O_4(^3\Sigma_g^- \cdot {}^1\Delta_g)$ with the fixed step $\Delta R = 0.2$ Å with the optimization of all other structural parameters (in the region of the most important portions of the energy curves; e.g., near the equilibrium distance, the step was decreased to ΔR(O2–O3) = 0.05 Å).

According to the principle of chemical reaction reversibility, the calculated PEC also corresponds to the optimal pathways for reactants approaching each other in the reaction $^3O_2(^3\Sigma_g^-) + {}^1O_2(^1\Delta_g) \longrightarrow {}^3O_4(^3\Sigma_g^- \cdot {}^1\Delta_g)$. Such a calculation procedure makes it possible to choose the minimal-energy pathway orientations of reactants.

The precision values of the activation barriers, dissociation energy, and the structural parameters for the dissociation of $^3O_4(^3\Sigma_g^- \cdot {}^1\Delta_g)$ were calculated taking into account the electron correlation energy using the method of complete active space self-consistent field (CASSCF). The use of this method is necessary for the correct description of the symmetry of wave function of the $^3O_4(^3\Sigma_g^- \cdot {}^1\Delta_g)$ molecule, because systems containing singlet dioxygen cannot be described correctly in the framework of the methods that use a one-determinant wave function. The calculation of the $^3O_4(^3\Sigma_g^- \cdot {}^1\Delta_g)$ molecule was carried out in the 6-311+G(d,p) basis set for the active space involving eight electrons and eight orbitals (henceforth, denoted as (8,8)) with the optimization of all its geometric parameters. The calculations of molecules $^3O_2(^3\Sigma_g^-)$ and $^1O_2(^1\Delta_g)$ were also carried out using the CASSCF method in the 6-311+G(d,p) basis set and the active space (4,6) with the optimization of interatomic distance. The choice of this active space for the calculation of the $^3O_2(^3\Sigma_g^-)$ and $^1O_2(^1\Delta_g)$ molecules is explained by the fact that it is necessary to involve the same orbitals in the active space as for the $^3O_4(^3\Sigma_g^- \cdot {}^1\Delta_g)$ molecule. This makes it possible to calculate all molecules participating in the dissociation reaction with the same accuracy $^3O_4(^3\Sigma_g^- \cdot {}^1\Delta_g) \longrightarrow {}^3O_2(^3\Sigma_g^-) + {}^1O_2(^1\Delta_g)$. The values of the activation barrier of the transition from the *twist* to *trans* configuration was refined in the framework of the CASSCF methods in the active space (8,8) with the geometry obtained by the UHF method in the 6-311+G(d,p) basis set.

The $HO_4^{\cdot}$ and $OOH^{\cdot}$ radicals were calculated by the G2 method, which has approximately the same accuracy as CASSCF but requires less computation. Calculations were carried out using Gaussian 94.

RESULTS AND DISCUSSION

The photophysical method for generating singlet dioxygen $^1O_2(^1\Delta_g)$ via energy transfer from an excited photosensitizer molecule to $^3O_2$ is used most frequently [24]. Chemical reactions are also known that result in the formation of dioxygen in the singlet state as, for instance, the recombination of peroxy radicals [25], the oxidation of the HO_2^- ion by the hypochlorite ion in aqueous alkali solutions [26], and the reaction of superoxide radical ion with halogenated hydrocarbons [27]. Recently, a new method has been developed for generating $^1O_2(^1\Delta_g)$ using the catalytic decomposition of alkyl hydroperoxides [28] or hydrogen peroxide [14–18, 29, 30] with the formation of active species capable of generating $^1O_2$ or transferring it to the substrates:

$$2H_2O_2 \xrightarrow{Cat} {}^1O_2 + 2H_2O,$$

where Cat = $Ca(OH)_2$, H_2TiO_3, $NaVO_3$, Na_2MoO_4, Na_2WO_4, etc.

In this work we used $VO(acac)_2$ in acetic acid and Na_2MoO_4 in water as catalysts.

1. Anomalous Line Broadening in EPR Spectra of Free Radicals

When hydrogen peroxide decomposes in acetic acid in the presence of vanadium(V) complexes, several active diamagnetic intermediates (various oxygen-containing vanadium complexes) are formed [14–18]. In addition to these compounds, a paramagnetic species was found in the system under consideration. Its EPR spectrum in the argon atmosphere is a well-resolved octet with $g = 2.01125 \pm 0.00005$ and $a = 4.8$ G (a is the hyperfine interaction constant). The spectral parameters of the observed signal coincide with the parameters of the vanadium(V) complex with the superoxide radical ion $V^{(V)}(O_2^-)$ described above [31–33]. In the absence of argon purging, the EPR lines of this complex radical are broadened from 2.6 to 6–8 G without changing their integral intensity. The spectral parameters of EPR lines for nitroxyl radicals **1** and **2** in the cat-

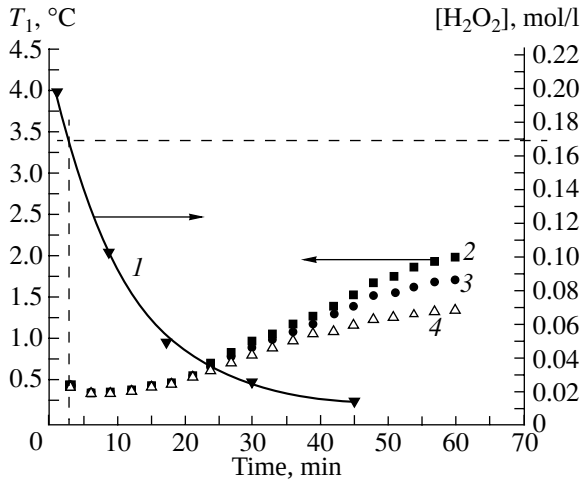

Fig. 3. Decomposition of H_2O_2 catalyzed by (*1*) Na_2MoO_4 and the relaxation times (T_1) of (*2*) water protons, (*3*) protons of sodium acetate, and (*4*) protons of sodium pilavate. $[Mo^{(VI)}] = 10^{-2}$ mol/l, $[H_2O_2]_0 = 0.22$ mol/l, $T = 30°C$; phosphate buffer (pH 10.5).

alytic systems $V^{(V)}/H_2O_2/AcOH$ and $Mo^{(VI)}/H_2O_2/D_2O$ change in an analogous manner.

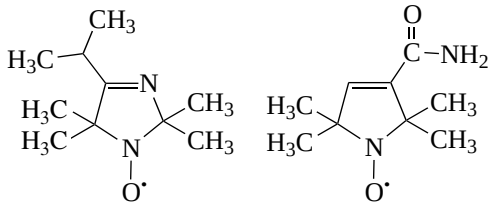

1 **2**

For the acetic acid system, radical **1** was chosen, which is rather stable in an acidic medium, and this made it possible to monitor the change in the form of the EPR signal in the course of the reaction.

In the absence of hydrogen peroxide in the EPR spectrum of a 10^{-4} M solution of radical **1** in $V^{(V)}$/AcOH, a characteristic triplet (g = 2.0028 G) is observed. After introducing 1 M H_2O_2, the EPR spectrum of the reaction mixture in a flow of argon is a superposition of two signals, an octet corresponding to $V^{(V)}(O_2^-)$, and a triplet corresponding to the nitroxyl radical **1**. Both signals are well resolved (in an argon atmosphere for radical **1**: α = 1.20–1.32 G, a = 14.5 ± 0.1 G; for $V^{(V)}(O_2^-)$: α = 0.94–1.15 G; α is the linewidth and a = 4.8 G). If the solution is not purged with any gas after ~2 min, both signals are broadened (by more than 7 G) so that a cannot be determined due to the small amplitude of the signal for **1**. For $V^{(V)}(O_2^-)$, the parameters of the spectrum are $\alpha \sim 5.14$ G, and $a \sim 4.9$ G. When purging is resumed, the initial form of the spectrum and the values of parameters of both signals are restored.

In the $Mo^{(VI)}/H_2O_2/D_2O$ system, the decomposition of hydrogen peroxide occurs via the molecular mechanism, and according to EPR data, does not result in the formation of paramagnetic species even in side reactions. Our experiments showed that nitroxyl radical **2** is not consumed in the H_2O_2 decomposition in the $Mo^{(VI)}/H_2O/D_2O$ system.

In the absence of hydrogen peroxide, the EPR spectrum of a 10^{-4} M solution of radical **2** in $Mo^{(VI)}/D_2O$ ($[Mo^{(VI)}] = 10^{-2}$ M) contains a triplet (g = 2.0049, a = 15.49 G) with a linewidth of 1.52 G in the case of argon purging. When the same solution is purged with triplet O_2, line broadening is minor (up to 2.50 G). After adding 1 M H_2O_2 without purging, the EPR signal of nitroxyl radical **2** immediately broadens (the spectrum was recorded 2–3 min after reactant mixing) up to a certain value (~8.3 G). The values of the g factor, a, and the integral intensity are preserved. Purging the reaction solution with argon narrows the spectrum to the initial parameters. Such line broadening and narrowing can be observed many times during the period while H_2O_2 is present in the system.

The constancy of the g factor, a, and the integral intensity under different conditions of spectrum recording points to the fact that both narrow and broad signals of the EPR spectrum correspond to the same paramagnetic species. The value line broadening is independent of the nature of the radical, catalyst (vanadium or molybdenum), and the medium where the reaction occurs (acidic for vanadium and alkali for molybdenum).

Narrowing the spectral lines when purging the reaction solution by any gas (argon, CO_2, or $^3O_2$) points to the fact that a volatile product accumulated in H_2O_2 decomposition is responsible for the unusual EPR line broadening. It is possible that such a substance is dioxygen formed in H_2O_2 decomposition, because this is the only known gaseous product formed in the $Mo^{(VI)}/H_2O_2/H_2O$ system.

2. Analysis of Possible Reasons for Anomalous EPR Line Broadening

2.1. Solution oversaturation with triplet dioxygen. Experiments requiring exact measurements of linewidth in the EPR spectrum were carried out in the $Mo^{(VI)}/H_2O_2/H_2O$ system because the linewidth of the well-resolved triplet of nitroxyl radical **2** can be measured rather accurately in the case of a line broadening of 7–10 G. The complex radical $V^{(V)}(O_2^-)$ is always present in a stationary concentration in the $V^{(V)}/H_2O_2/AcOH$ system (see above), and its spectrum loses its fine structure when the spectrum broadens. This makes accurate measurements impossible.

In the Mo(Vl)-catalyzed decomposition of hydrogen peroxide, broadening is observed for at least 40 min. During this period, 70–90% of hydrogen peroxide is decomposed. The widths of EPR lines decrease

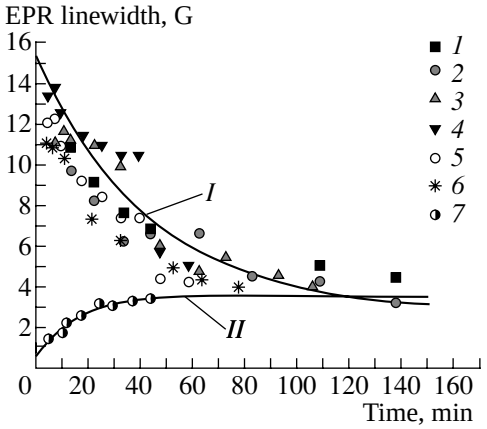

Fig. 4. A change in the EPR linewidth of radical **2** in H_2O_2 decomposition in the (*I*) $Mo^{(VI)}/H_2O_2/H_2O$ and (*II*) $Fe^{(II)}/H_2O_2/H_2O$ systems. T = 20°C. (*I*): at $[Mo^{(VI)}] = 10^{-2}$ mol/l: (*1*) $[\mathbf{2}] = 5 \times 10^{-3}$ mol/l, (*2*) $[\mathbf{2}] = 10^{-3}$ mol/l, (*3*) $[\mathbf{2}] = 10^{-4}$ mol/l; at $[\mathbf{2}] = 10^{-4}$ mol/l: (*4*) $[Mo^{(VI)}] = 2 \times 10^{-2}$ mol/l, (*5*) $[Mo^{(VI)}] = 5 \times 10^{-2}$ mol/l, (*6*) in the presence of 10^{-3} mol/l NaN_3. $[H_2O_2]_0$ = 0.2 mol/l, phosphate buffer (pH 10). (*II*): $[Fe^{(II)}] = 10^{-2}$ mol/l, $[H_2O_2]_0$ = 1 mol/l, $[\mathbf{2}] = 5 \times 10^{-4}$ mol/l, KOH solution, pH 10.

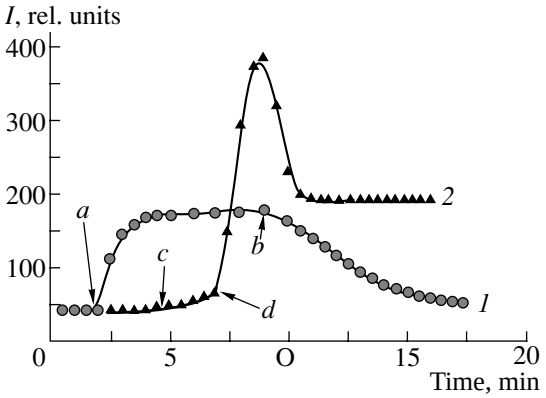

Fig. 5. Dependence of the concentration of dissolved oxygen on time: (*1*) in buffer solution purging with triplet dioxygen, (a) beginning of purging, (b) end of purging; phosphate buffer, pH 10.5, T = 25°C; (*2*) in hydrogen peroxide decomposition, (c) addition of H_2O_2 to the cell, (d) addition of the catalyst solution; $[Mo^{(VI)}] = 10^{-3}$ mol/l, $[H_2O_2]_0$ = 0.05 mol/l, phosphate buffer, pH 10.5, T = 25°C.

in a similar manner as H_2O_2 is consumed (Fig. 3, curve *1* and Fig. 4, curve *I*) and approaches a value corresponding to the widths of lines in an aqueous solution saturated with dioxygen ($^3O_2$) at a partial pressure of 1 atm (Fig. 4, curve *I*).

A general property of the catalytic systems for the decomposition of hydrogen peroxide where the effect described above is observed is their capability of generating dioxygen in the ground triplet ($^3O_2$) and excited ($^1O_2$, $^1\Delta_g$) states [14–18, 29, 30].

In connection with this, two hypotheses as to the reasons for anomalous broadening have been advanced:

(a) The effect is due to the accumulation of $^3O_2$ in the solution. It is the overequilibrium concentration of $^3O_2$ that has been used to explain ^{1}H NMR line broadening under conditions of H_2O_2 decomposition under the action of an electron beam [34]. In principle, the oversaturation of the solution with $^3O_2$ and the interaction of this paramagnetic species with the radical could be the reason for the apparent anomalous line broadening in the EPR spectra under the conditions of our experiments on the catalytic decomposition of H_2O_2 [14–18].

(b) The reason for the EPR line broadening is the presence of singlet oxygen in the solution.

To check these hypotheses, we carried out the following studies. The kinetics of EPR line broadening was compared with changes in the concentrations of triplet and singlet dioxygen in the course of the reaction using the most reliable methods to record them: the polarographic detection of $^3O_2$ [19] and the detection of $^1O_2(^1\Delta_g)$ using its proper chemiluminescence in the range of 1270 nm [21–24].

To determine the solubility of $^3O_2$ under the conditions used, oxygen was passed through a solution in a measuring cell while the concentration of oxygen grew until reaching the equilibrium value. When oxygen purging is discontinued, the concentration of dissolved O_2 starts to decrease and returns its initial value corresponding to the equilibrium of the solution with air for ~10 min (Fig. 5, curve *1*).

In the absence of the catalyst, the decomposition of hydrogen peroxide occurs very slowly and cannot be detected by the usual chemical methods. However, a change in the electrode potential pointed to detectable oxygen evolution, apparently due to hydrogen peroxide decomposition on the metallic wall of the measuring cell. This fact points to the high sensitivity of the method (Fig. 5, curve *2*). After adding the catalyst, intensive hydrogen peroxide decomposition begins and the concentration of dissolved oxygen dramatically increases and reaches the maximal value in 1.5–2 min (Fig. 5, curve *2*). Approximately 3 min after the beginning of decomposition, the concentration of oxygen dissolved in the reaction mixture decreased to a value that is close to equilibrium (at an oxygen partial pressure of 1 atm; Fig. 5, curve *2*). The maximal apparent concentration of dissolved oxygen is at most two times higher than the equilibrium one (at an oxygen partial pressure of 1 atm). The equilibrium concentration of dissolved oxygen restored after reaching the maximum earlier than the recording of the first EPR spectrum began.[1]

[1] The spectrum recording began 3–4 min after reactant mixing.

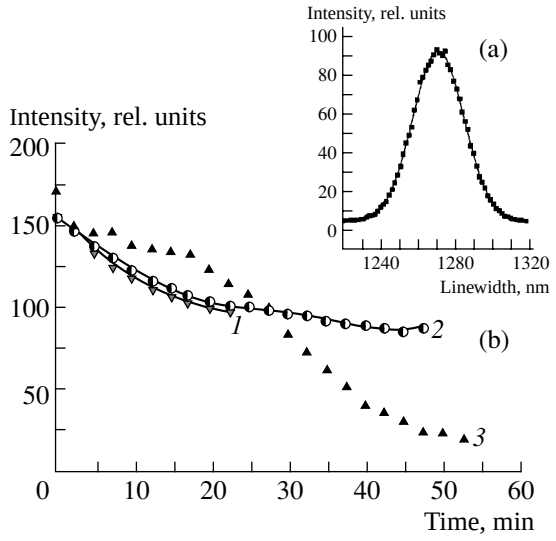

Fig. 6. (a) Chemiluminescence spectrum of singlet dioxygen obtained by the decomposition of hydrogen peroxide in the acetic acid solution. H_2O_2 = 1 mol/l, $[V^{(V)}] = 10^{-2}$ mol/l, T = 15°C; (b) dependence of the intensity at the maximum of chemiluminescence of singlet dioxygen on time in the decomposition of hydrogen peroxide in the systems (*1*, *2*) $V^{(V)}/H_2O_2$/AcOH and (*3*) $Mo^{(VI)}/H_2O_2/H_2O$ (*1*) in the absence and (*2*) in the presence of 2-ethylanthracene. $[H_2O_2]$ = 0.25 mol/l, [2-EA] = 0.02 mol/l, $[V^{(V)}] = 10^{-2}$ mol/l, T = 22°C. $[H_2O_2]_0$ = 0.17 mol/l, $[Mo^{(VI)}] = 10^{-3}$ mol/l, phosphate buffer, pH 10.5, T = 27°C.

As can be seen from Fig. 3, in the experiments on the catalytic decomposition of H_2O_2, EPR line broadening was observed immediately after adding hydrogen peroxide or the catalyst to the solution and continued for at least 40 min after the beginning of the reaction, that is, much later than the drop of $^3O_2$ concentration to the equilibrium value.

Note that all measurements of dissolved O_2 evolved in the decomposition of H_2O_2 were carried out under conditions of stirring.[2] We supposed that stirring might prevent the oversaturation of the solution with oxygen. However, our experiments showed that this was not the case. In contrast to our expectations, in the absence of stirring, the instrument showed an underestimated (by ~1.5%) concentration of dioxygen both at the maximum of the O_2 accumulation curve and at a portion of the curve that corresponds to solution saturation with oxygen and coincides with the EPR spectrum recording in time. It also follows from this observation that dioxygen formed in the reaction cannot be accumulated in the solution at a concentration that is an order of magnitude higher than the equilibrium concentration.

Under conditions of catalytic H_2O_2 decomposition by iron ions (1 mol/l H_2O_2, 10^{-2} mol/l $FeSO_4$, KOH solution, pH 10) when triplet dioxygen is intensively generated in the solution and singlet dioxygen is not formed [5], the maximal width of the EPR line of nitroxyl radical is 2.7–3.0 G, which corresponds to the paramagnetic broadening of the EPR line in the solution saturated with triplet dioxygen.[3] Moreover, the value of broadening increases with time (Fig. 4, curve *II*) and with an increase in the concentration of dissolved dioxygen, whereas in the H_2O_2 decomposition in the $V^{(V)}$/AcOH and $Mo^{(VI)}/H_2O$ systems, the linewidth in the EPR spectrum was maximal at the very beginning of a run (Fig. 4, curve *I*).

All these facts exclude the oversaturation of the solution with $^3O_2$ from a list of possible reasons behind the anomalous line broadening in the EPR spectra of radials.

To elucidate the possible effect of singlet dioxygen on EPR line broadening, we carried out experiments on IR chemiluminescence measurements of singlet dioxygen in the decomposition of hydrogen peroxide in the $V^{(V)}$/AcOH and $Mo^{(VI)}/H_2O$ systems. We found chemiluminescence with a spectral maximum at 1270 nm corresponding to the chemiluminescence of singlet dioxygen (Fig. 6a). The time interval of chemiluminescence decay approximately corresponds to the time interval of hydrogen peroxide decomposition, but the kinetics of these processes are different. The curve of H_2O_2 decomposition is adequately described by the monotonic monoexponential function $\frac{d[H_2O_2]}{dt} = -k[H_2O_2]_0e^{-kt}$. In the acetic acid solution of vanadium(V), the intensity of $^1O_2$ chemiluminescence also decreases exponentially (Fig. 6b, curve *3*), whereas chemiluminescence decays nonexponentially in the $Mo^{(VI)}/H_2O$ system, which is an indication of the complex nature of the process responsible for the apparent emission. Because the reaction is accompanied by the active formation of dioxygen bubbling through a layer of the liquid phase, it is possible that the chemiluminescence kinetics becomes more complex compared to the kinetics of hydrogen peroxide decomposition due to the superposition of the process of bubble formation and the process of singlet dioxygen redistribution between the gas phase and the solution. This idea correlates with the fact that the passage of triplet dioxygen through the reaction system eliminates line broadening in the EPR spectra of radicals [14–18]. The lifetime of singlet dioxygen in water is short, ~3 μs [23]. In acetic acid, this value is 23 ± 1 μs [17]. Thus, the removal of $^1O_2$ from the solution in the course of purging is only possible if the concentration of singlet dioxygen is determined by the equilibrium between the solution and the

[2] In our experiments, the reaction mixture was prepared in a test tube, vigorously stirred, and then poured into an EPR spectrometer cell.

[3] The rate of H_2O_2 decomposition in these experiments was the same as in the experiments with $Mo^{(VI)}$.

bubble gas phase, where the lifetime of singlet dioxygen is several orders of magnitude longer than in the solution [24].

It follows from Fig. 3 that H_2O_2 is almost entirely consumed for less than 1 h under the conditions of our experiments. However, it is noticeable that, even after H_2O_2 exhaustion and the cessation of $^1O_2$ generation, the EPR lines remain 1.5–2 times broader than in the solution saturated with triplet dioxygen (see curves *I* and *II* in Fig. 4 at $t = 1$ h).

The linewidth of ^{1}H NMR of water protons and protons of the CH_3 group in sodium acetate under conditions of $^1O_2(^1\Delta_g)$ formation in the $Mo^{(VI)}/H_2O_2/H_2O$ system increases more than 100 times. Thus, before adding hydrogen peroxide, it is ~0.8 Hz, whereas in the course of H_2O_2 decomposition it is ~100 Hz. The relaxation time of protons T_1 under these conditions decreases more than 10 times: from 5.98 ± 0.08 to 0.412 ± 0.08 s for the protons of the CH_3 group and from 11.3 ± 0.1 to 0.442 ± 0.09 s for water protons (Fig. 3, curves *2–4*).

After a drastic decrease at the beginning of the run and passing through a poorly resolved maximum, the value of T_1 begins to increase long before the end of H_2O_2 decomposition. However, the relaxation time does not reach the initial relaxation time of protons T_1 even ~48 h after exhaustion H_2O_2.

To elucidate the reason behind ^{1}H NMR line broadening, we measured the relaxation times of protons of water, sodium acetate, and sodium pivalate in a buffer solution (D_2O, pH 10.5) in the presence and in the absence of $Mo^{(VI)}$ complexes at oxygen pressures P_{O_2} ranging from 0.2 to 6 atm at 30°C. The presence of a catalyst appeared to affect the value of T_1 insignificantly.

The resulting data are well described by a straight line in the coordinates $1/T_1 - P_{O_2}$ (Fig. 7). These data can be used to estimate the concentration of $^3O_2$ in the solution. Thus, the first measurement of the value of T_1 3 min after the beginning of H_2O_2 decomposition showed that the relaxation times of all protons decreased to ~0.4 s (Fig. 3, curves *2–4*). It is seen from Fig. 6 that such a value of T_1 is observed at an oxygen pressure of 12 ± 2 atm, that is, at the concentration of dissolved dioxygen $(1.35 \pm 0.23) \times 10^{-2}$ M (the equilibrium solubility of O_2 in water is $\sim 3.6 \times 10^{-2}$ g/l at 30°C and 1 atm [35]). By that time, 0.03 M of hydrogen peroxide decomposed. That is, provided that the dioxygen formed remained entirely in the solution, its concentration reached 1.5×10^{-2} M. Thus, assuming that if the dioxygen formed remains entirely in the solution, its concentration should be sufficient to reach the apparent relaxation time. In fact, a considerable portion of dioxygen desorbs and the above condition is not fulfilled. Nevertheless, we may reasonably assume that the effect observed in the NMR spectra is largely due to the oversaturation of the solution with $^3O_2$.

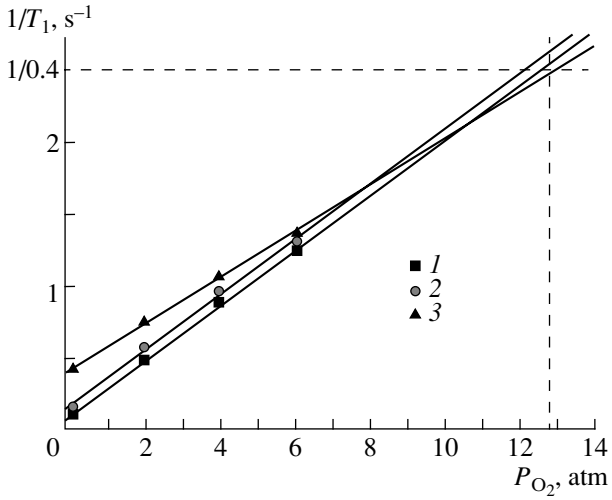

Fig. 7. Dioxygen pressure dependence of the reciprocal relaxation time ($1/T_1$) of protons of (*1*) H_2O, (*2*) CH_3COONa, and (*3*) $(CH_3)_3CCOONa$. $T = 30$°C, phosphate buffer, pH 10.5.

All the experimental curves considered above can be categorized according to their shapes: the first group involves H_2O_2 decomposition (Fig. 3, curve *1*), $^1O_2$ chemiluminescence decay (Fig. 6b), and a decrease in the EPR linewidth in the $Mo^{(VI)}/H_2O$ system with time (Fig. 4, curve *1*). Comparison of these curves shows that all three processes are cymbate. The values monotonically decrease from the maximal value at the beginning of a run to the minimal value at the end.

The other category of curves includes the accumulation of dissolved triplet dioxygen in the decomposition of H_2O_2 (Fig. 5, curve *1*), a change in the width of the EPR line in the $Fe^{(II)}/H_2O_2/H_2O$ system (Fig. 4, curve *II*), and a decrease in T_1 of protons (Fig. 3, curves *2–4*). These curves also correlate with each other. Thus, the maximum concentration of $^3O_2$, the width of the EPR line for radical **2**, and the minimum of the relaxation time are achieved not immediately but after a certain period from the beginning of the experiment. Note that the EPR linewidth of radical **2** in the $Fe^{(II)}/H_2O_2/H_2O$ system reaches the stationary values after ~40 min, that is at the end of the H_2O_2 decomposition reaction, whereas the value of T_1 slowly (over a day) approaches the initial value. These effects are due to the presence of triplet dioxygen in the system.

Our data point to the fact that the reasons for the decrease in the proton nucleus relaxation time observed in the NMR spectrum and the anomalous line broadening in the EPR spectrum are different. Thus, the maximal line broadening in the EPR spectrum is observed right after the beginning of $^1O_2$ evolution, whereas the poorly resolved maximum of the effect (the minimal value of T_1) registered in the ^{1}H NMR spectra is observed after a certain period of time (Fig. 3, curves *2–4*). The linewidths of the EPR signal drastically decrease by the end of the run when the values of T_1 slowly

increase and do not reach the initial value even after H_2O_2 exhaustion.

The antibatic nature of curves belonging to different categories points to the fact that triplet dioxygen is not the only agent responsible for the broadening of EPR signals of paramagnetic species and suggests that the anomalous line broadening is associated with the formation of singlet dioxygen in the solution.

Diamagnetic species $^1O_2$ is hardly capable of affecting the shape of EPR spectra. However, singlet dioxygen or its complex may participate in the formation of a relatively stable paramagnetic species.

2.2. Formation of dimeric O_4 species The existence of triplet dioxygen dimers is known from the literature.[4] This species was detected in the gas phase at a low temperature [37] and in a neon matrix [38] by spectral methods and by molecular beam scattering [39]. The ability of $^1O_2$ molecules to form O_4 dimers ("dimoles" [24, 40]) is also known. In connection with this, the question arises as to whether a reaction between $^1O_2$ and $^3O_2$ is possible with the formation of biradical species capable of contributing to the EPR line broadening. Indirect data pointing to the possibility of reactions between the singlet and triplet dioxygen have been obtained in the photoionization of argon and oxygen mixtures [41]. Under these conditions, species with the compositions O_4^+ and O_6^+ have been identified. Their formation points to a reaction between $^1O_2$ and the paramagnetic cation O_2^+. Under conditions of mass spectrometric–chromatographic experiments, the addition of O_2^+ to O_2 also occurs with the formation of O_4^+. Adding an electron to this cation leads to the formation of a neutral O_4 molecule, which is registered in the mass spectrum after secondary ionization after a certain period [42].

One of the tasks of this work was to determine whether the addition of an $^3O_2$ molecule rather than the cation to the $^1O_2$ molecule is possible.

As early as in 1924, Lewis conjectured the existence of dimers (dimoles) of dioxygen O_4 [43], which have been studied since then because understanding the nature of bonding in such dimers forms the basis for the description of various processes. In 1960 Pauling proposed that van der Waals forces play the main role in the bonding in these molecules [44]. In 1966 Leckenby and Robbins published the first mass spectrometric evidence for the existence of such dimers in gaseous oxygen at normal temperatures and pressures [45]. Earlier, they found the dimers of triplet dioxygen in the course of ultrasonic adiabatic gas outflow from a reservoir (40 atm) into a high vacuum [46].

It is commonly believed that the interaction of dioxygen molecules $^3O_2$ in the gas phase leads to three types of dimers $(O_2)_2$: collision pair, metastable, and "bound" states [47]. The binding in these molecules is hundreds of times weaker than in usual chemical compounds. The estimated energy of the $^3O_2$–$^3O_2$ bond is 0.46 kcal/mol [48]. In experimental searches for the $^3O_2$–$^3O_2$ dimers, weak absorption in the infrared, red (near 630 and 580 nm), blue, and near UF regions was detected [49]. In the study of absorption spectra of thin (<0.5 μm) samples of the "red phase" of solid oxygen at high pressures (up to 63 MPa), a new mighty peak was observed at ~300 cm^{-1}. According to the authors, the nature of the spectrum points to the association of oxygen molecules leading to the formation of O_4 [50].

The energy of $^3O_2$–$^3O_2$ formation estimated from the IR absorption spectra is 0.83 kcal/mol [51].

A more exact quantum chemical characteristic of the nature of $^3O_2$–$^3O_2$ interaction gives the binding energy of the ground (singlet) state of the O_2–O_2 dimer: 17.0 ± 0.8 meV for the most stable geometry: two oxygen molecules parallel to each other at a distance of 3.56 ± 0.07 Å [36]. This typical value of the energy of weak van der Waals interaction correlates with the distance found in the dimmer. A further decrease in the distance between the molecules leads to a rapid increase in the energy of the system.

The phosphorescence of dimole singlet dioxygen $[O_2(^1\Delta_g)]_2$ was discovered as early as in 1927 in the study of chemiluminescence that appears in the reaction of hydrogen peroxide with NaClO [52]. More recently, it has been found that the maximum of the chemiluminescence spectrum is near 634 nm [53]. The spectrum also contains bands at 580, 703, 760, 860, 1070, and 1270 nm [26, 54, 55]. Spectral and kinetic data led the authors of those studies to the conclusion that in all cases the dimers $[O_2(^1\Delta_g)]_2$ are responsible for luminescence in the region of <760 nm. Initially, this luminescence was only observed in the gas phase, but later luminescence of $[O_2(^1\Delta_g)]_2$ was also observed in liquid oxygen [56] and in the solutions under the action of direct laser excitation of O_2 dissolved in fluorinated solvents [57] and in air-saturated solutions in the photosensitized generation of $O_2(^1\Delta_g)$ [22, 58–60].

There is preliminary quantum chemical information on the structure of molecular oxygen dimers consisting of $[O_2(^1\Delta_g)]_2$ and $[O_2(^3\Sigma_g^-)]_2$, whereas data on dimole O_4 or the $O_2(^1\Delta_g)O_2(^3\Sigma_g^-)$ molecule are absent. Probably, the problem of energetics and the structure of such adducts has never been posed.

According to our quantum chemical calculations, the values of the activation barriers taking into account the electron correlation energy are 1.1 kcal/mol for the twist to *trans* transition and 4.7 kcal/mol for the *twist* to *cis* transition.

[4] The term dimer of triplet dioxygen does not refer to the O_4 molecule but rather to a pair of triplet dioxygen molecules $(O_2)_2$ the distance between which is 2.5–5 Å. The existence of such a dimer is largely due to the van der Waals forces, but the contribution from the chemical spin–spin interaction cannot be neglected since it constitutes ~15% of the van der Waals interaction [36].

Table 1. Geometry of the molecule $O_4(^3\Sigma_g^- \cdot {}^1\Delta_g)$ in the equilibrium configuration obtained in the approximations UHF/6-311+G(d, p) and CASSCF/6-311+G(d, p)

Parameter	*Trans* conformation ($^3B_{3g}$)		*Twist* conformation ($^3A_1$)	
	UHF	CASSCF(8,8)	UHF	CASSCF(8,8)
R(O1–O2), *R*(O3–O4)	1.2512 Å	1.3100 Å	1.2672 Å	1.336 Å
R(O2–O3)	1.4198 Å	1.5739 Å	1.3874 Å	1.4910 Å
φ(O3O2O1), φ(O4O3O2)	107.1°	104.3°	109.7°	107.0°
φ(O4O3O2O1)	180.0°	180.0°	81.7°	84.9°
Energy, a. u.	−299.192219	−299.305471	−299.193639	−299.306480

The results of PEC calculation for the dissociation of $^3O_4(^3\Sigma_g^- \cdot {}^1\Delta_g)$ are shown in Table 1. The difference in the geometric parameters obtained by the CASSCF and UHF methods is at most ±10%. Figure 8 shows PECs corresponding to the dissociation of $^3O_4(^3\Sigma_g^- \cdot {}^1\Delta_g)$ in the *trans* and *twist* conformations. These are the curves showing changes in the potential energy of the system depending on the *R*(O2–O3) distance in a $^3O_4(^3\Sigma_g^- \cdot {}^1\Delta_g)$ molecule.

The results showed that the values of *R*(O1–O2) and *R*(O4–O3) in the region of the dissociation of the $^3O_4(^3\Sigma_g^- \cdot {}^1\Delta_g)$ molecule are close to the experimental value *R*(O–O) = 1.2075 Å in the isolated dioxygen molecule (1.170 Å in our calculation).

The results of calculation of the energies of the molecules $^3O_2(^3\Sigma_g^-)$, $^1O_2(^1\Delta_g)$, and $^3O_4(^3\Sigma_g^- \cdot {}^1\Delta_g)$ show (Table 2) that the value of the full energy of the system $^3O_4(^3\Sigma_g^- \cdot {}^1\Delta_g)$ with the equilibrium geometry and in the dissociation limit virtually coincide with the sum of the full energies of isolated reactants $^3O_2(^3\Sigma_g^-)$ and $^1O_2(^1\Delta_g)$ (the difference is as small as ±0.003 atomic units). This led us to the conclusion that the parameters of the active space were chosen correctly for the molecules $^3O_4(^3\Sigma_g^- \cdot {}^1\Delta_g)$, $^3O_2(^3\Sigma_g^-)$, and $^1O_2(^1\Delta_g)$ and that the calculated dissociation energies are rather accurate.

Twist and *trans* conformations of the $^3O_4(^3\Sigma_g^- \cdot {}^1\Delta_g)$ molecule correspond to the shallow local minima on the corresponding PECs: 1.97 and 0.54 kcal/mol (Fig. 8). Thus, the endothermic $^3O_4(^3\Sigma_g^- \cdot {}^1\Delta_g)$ molecule may exist in the form of a snake. Shallow potential wells characterize the $^3O_4(^3\Sigma_g^- \cdot {}^1\Delta_g)$ molecule as unstable despite the stability of the Hartree–Fock solution.

It follows from the data obtained that, for the formation of the $^3O_4(^3\Sigma_g^- \cdot {}^1\Delta_g)$ molecule in the *twist* and *trans* conformations from the $^3O_2(^3\Sigma_g^-)$ and $^1O_2(^1\Delta_g)$ and molecules, 18.6 and 18.9 kcal/mol should be expended (Fig. 8). Thus, in the absence of an additional energy source, the reaction between the triplet and singlet dioxygen molecules is thermodynamically unfavorable.

However, we cannot exclude the reaction

$$2H_2O_2 + {}^3O_2(^3\Sigma_g^-) \longrightarrow {}^3O_4(^3\Sigma_g^- \cdot {}^1\Delta_g) + 2H_2O. \quad (I)$$

The metathesis of hydrogen peroxide with the formation of singlet dioxygen provides energy which is almost equivalent to the energy of the endothermic reaction of $^1O_2(^1\Delta_g)$ with $^3O_2(^3\Sigma_g^-)$:

$$2H_2O_2 \longrightarrow 2H_2O + {}^1O_2(^1\Delta_g)$$

$$\Delta G^\circ_{298} = -24 \text{ kcal/mol}.$$

Kinetic studies of hydrogen peroxide metathesis

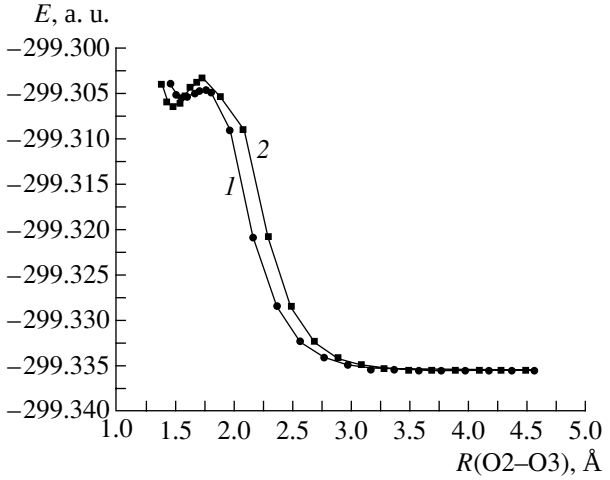

Fig. 8. Dissociation curves of the $O_4(^3\Sigma_g^- \cdot {}^1\Delta_g)$ molecule into $^1O_2(^3\Sigma_g^-)$ and $^3O_2(^1\Delta_g)$ for (*1*) *trans* and (*2*) *twist* configurations depending on the *R*(O2–O3) distance estimated by the CASSCF method.

Table 2. Full energies (a. u.) of the $^3O_4(^3\Sigma_g^- \cdot {}^1\Delta_g)$ molecule in the equilibrium configuration and at the dissociation limit and full energies of the molecules $^3O_2(^3\Sigma_g^-)$ and $^1O_2(^1\Delta_g)$ obtained by the CASSCF method (the basis set 6-311+G(d, p))

Method	$^3O_4(^3\Sigma_g^- \cdot {}^1\Delta_g)$	
	trans conformation	*twist* conformation
CASSCF(8,8)	–299.305471	–299.306480
CASSCF(8,8) (dissociation limit)	–299.335610	–299.335610

	$^3O_2(^3\Sigma_g^-)$	$^1O_2(^1\Delta_g)$	$^3O_2(^3\Sigma_g^-) + {}^1O_2(^1\Delta_g)$
CASSCF(8,8)	–149.646623	–149.685531	–299.332154

catalyzed by vanadium(V) compounds and anthracene oxidation under the conditions of this reaction suggested that the anthracene molecule, which plays the role of a singlet dioxygen trap, reacts with a vanadium(V) complex and accepts the $^1O_2(^1\Delta_g)$ molecule formed [61–64]. We cannot exclude that the role of the $^1O_2(^1\Delta_g)$ molecule acceptor can belong to triplet dioxygen *in statu nascendi*. In the framework of this approach, the oversaturation of the $^3O_2(^3\Sigma_g^-)$ solution should be favorable for an increase in the concentration of $^3O_4(^3\Sigma_g^- \cdot {}^1\Delta_g)$.

Comparison of the curves of chemiluminescence decay for $^1O_2$ formed in the $V^{(V)}/H_2O_2$/AcOH system with and without 2-ethylanthracene (Fig. 6b, curves *1*, *2*) showed that the initial luminescence intensity and the rate of its decrease are virtually the same; that is, the steady-state concentration of singlet dioxygen does not decrease with the addition of 2-ethylanthracene and remains ~10^{-7} mol/l. This observation confirms that free singlet dioxygen does not react with 2-ethylanthracene and points to the fact that the sources of singlet dioxygen and the active oxidant are different vanadium(V) complexes.

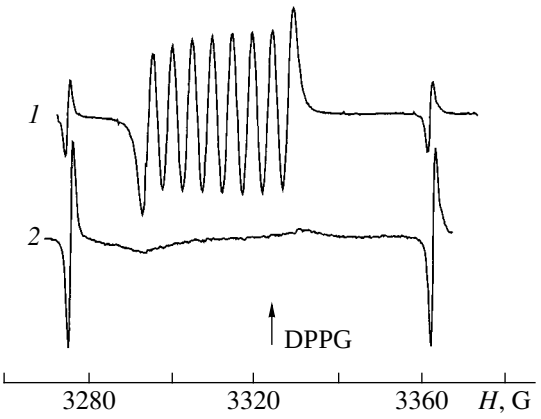

Fig. 9. EPR spectra of the superoxide radical ion $V^{(V)}(O_2^-)$ in the course of hydrogen peroxide decomposition in the $V^{(V)}/H_2O_2$/AcOH system (*1*) in the presence and (*2*) in the absence of 2-ethylanthracene.

In the experiments on the oxidation of 2-ethylanthracene, the EPR spectra of superoxide radical anion $V^{(V)}(O_2^-)$ are a well resolved octet with a linewidth of ~1 G (Fig. 9, spectrum *1*). The evolution of dioxygen into the volume in the decomposition of hydrogen peroxide in the presence of 2-ethylanthracene in high concentrations (~0.05 mol/l) is substantially reduced (Fig. 10): almost all the dioxygen that could be formed by H_2O_2 decomposition is spent on substrate oxidation. Under these conditions, a singlet dioxygen molecule formed inside the coordination sphere of the vanadium complex probably transfers onto the anthracene molecule rather than onto the molecule of triplet dioxygen. In this case, the steady-state concentration of $^3O_4(^3A_1)$ should decrease. Because in the framework of the given mechanism spectral line broadening should be assigned to the presence of $^3O_4(^3A_1)$ in the solution, we expect that, despite the high steady-state concentration of $^1O_2(^1\Delta_g)$ in the presence of 2-ethylanthracene, narrow

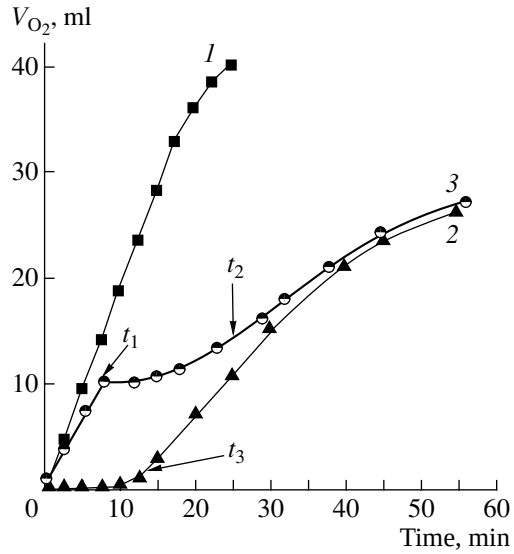

Fig. 10. Amount of oxygen V_{O_2} evolved in hydrogen peroxide decomposition in the $V^{(V)}/H_2O_2$/AcOH system (*1*) without 2-ethylanthracene, (*2*) when 2-ethylanthracene is added at the beginning of H_2O_2 decomposition, and (*3*) in the course of H_2O_2 decomposition. $[H_2O_2]$ = 1 mol/l, $[V^{(V)}] = 10^{-4}$ mol/l, [2-EA] = 0.05 mol/l, T = 50°C; t_1 is the time 2-ethylanthracene addition, t_2 and t_3 are the times of 90% conversion of 2-ethylanthracene.

lines should be observed in the EPR spectrum. The experiment is in excellent agreement with this conclusion based on the proposed mechanism.

It is characteristic that such an efficient quencher of singlet dioxygen as sodium azide does not affect the linewidth in the EPR spectra. It is seen from Fig. 4 that the linewidth of radical **2** is independent of the presence or absence of sodium azide in the solution (points *6* on curve *I*). This result becomes clear if we assume that EPR line broadening is largely determined by the concentration of $^3O_4(^3A_1)$ or any other adduct of singlet dioxygen with which the N_3^- ion does not react and on the concentration of which the N has no effect.

2.3. The formation of radicals $HO_4^\bullet$. The reactions of species with unpaired electrons to singlet dioxygen are possibly as typical for this compound as the formation of adducts with the compounds containing the systems of double bonds or an isolated C=C bond. Thus, according to quantum chemical calculation, the addition of a hydrogen atom to the $^1O_2(^1\Delta_g)$ molecule has no barrier and is exothermic [64]. Peroxy radicals are efficient physical quenchers of $^1O_2$ [10–12]. Stable nitroxyl radicals are also the quenchers of $^1O_2$, but the rates are lower [13]. We studied the addition of the $HO_2^\bullet$ radical to the $^1O_2(^1\Delta_g)$ by quantum chemical methods in connection with the problem of interaction of oxygen-centered free radicals with the $^1O_2(^1\Delta_g)$ molecule.

It is known [65] that the $HO_2^\bullet$ radical is stabilized by molecular orbitals orthogonal to the molecular plane by analogy with the dioxygen molecule. The radical $HO_3^\bullet$ containing three oxygen atoms is even more stable due to the ozone-like delocalization of π-MO. Longer radicals, including $HO_4^\bullet$, take a spiral form and this leads to a decrease in the stability of the two oxygen atoms at the ends of a chain. The energy of stabilization of radicals calculated in [65] are 64.4 kJ/mol for $HO_2^\bullet$, 88.7 kJ/mol for $HO_3^\bullet$, and 69.5 kJ/mol for $HO_4^\bullet$.

In the UHF/6-31G(d,p) approximation with full geometry optimization with the step ΔR(O2–O3) = 0.2 Å, PEC was calculated corresponding to the minimum energy pathway for the dissociation reaction $^\bullet OOOOH \longrightarrow {}^1O_2 + {}^\bullet OOH$ (Fig. 11). To obtain a precision value of the heat of the reaction of $^\bullet OOOOH$ formation (Fig. 1c) from $^1O_2$ and $^\bullet OOH$, we calculated $^1O_2$, $^3O_2$, $^\bullet OOH$, and $^\bullet OOOOH$ by the G2 method. Analysis of the data obtained shows that the value of singlet–triplet splitting in the O_2 molecule obtained by this method (23.9 kcal/mol) agrees well with experimental data [1].

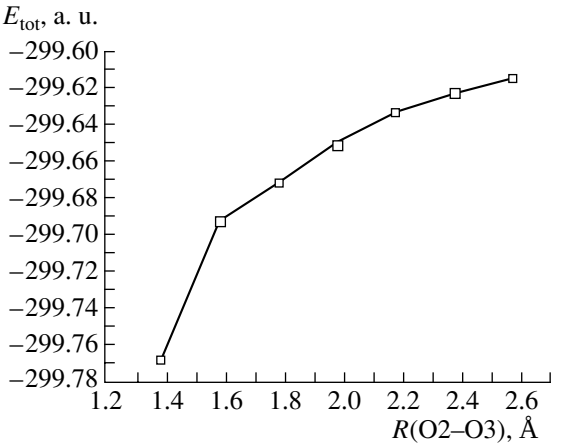

Fig. 11. Potential energy curve corresponding to the minimal energy path of the dissociation reaction $^\bullet OOOOH \longrightarrow {}^1O_2 + {}^\bullet OOH$.

The reaction $^1O_2 + {}^\bullet OOH \longrightarrow {}^\bullet OOOOH$ is slightly exothermic: ΔQ = 2.30 kcal/mol.

This result points to new pathways for singlet dioxygen transformations with the participation of paramagnetic species in alkali solutions, where, for instance, MoO_4^{2-} actively catalyzes the decomposition of H_2O_2 with the formation of $^1O_2(^1\Delta_g)$ [29, 30]. At the same time, this result can explain the pathways of $^1O_2(^1\Delta_g)$ quenching catalyzed by the peroxy radical. The barrier-free addition of the $ROO^\bullet$ radical to the $^1O_2(^1\Delta_g)$ molecule and the subsequent fast decomposition of the adduct with the generation of $ROO^\bullet$ and the formation of the $^3O_2(^3\Sigma_g^-)$ molecule may form the basis for fast quenching of $^1O_2(^1\Delta_g)$.

CONCLUSION

The goal of this work was to determine factors responsible for the experimentally observed anomalous broadening of signals from free radicals in the EPR spectra and changes in the nuclear relaxation times in the NMR spectra of electron-saturated compounds in the solutions $V^{(V)}/H_2O_2/AcOH$ and $Mo^{(VI)}/H_2O_2/H_2O$.

Our results suggest that anomalous line broadening in the EPR spectra observed in solutions where singlet dioxygen is chemically generated is only associated with the formation of this electronically excited molecule. This effect is at least in part due to the formation of such hypothetical species as biradical $^3O_4(^3A_1)$ and radical $^\bullet OOOOH$ in the system. According to quantum chemical estimates, the stability of these compounds in the gas phase is low. However, we think that such compounds can be stabilized due to the interaction with the

solvent molecules. Furthermore, we expect that the concentration of the biradical $^3O_4(^3A_1)$ would increase with an increase in the concentration of $^3O_2$ because of the oversaturation of the solution in the course of H_2O_2 decomposition.

Analysis of detailed mechanisms of EPR line broadening was beyond the scope of this work. This would require taking into account effects appearing in the course of $^1O_2$ quenching, times of spin–lattice relaxation of $^3O_4(^3A_1)$ and $^{\bullet}$OOOOH, and other line-broadening factors.

A change in the time of nuclear relaxation under the conditions of our experiments can be explained by the oversaturation of the $^3O_2$ solution if we make the unreasonable assumption that, in contrast to the experimental data, all of the $^3O_2$ formed in the system does not desorb from the solution. Nevertheless, the effect observed is, of course, at least partly due to the interaction of solvate nuclei with the $^3O_2$ molecules.

Results pointing to the possibility of formation of the biradical $^3O_4(^3A_1)$ are very important in connection with the discussion of the problems of the chemistry of singlet dioxygen.

ACKNOWLEDGMENTS

We thank Professor A.A. Krasnovskii for helpful discussions. This work was supported by the Russian Foundation for Basic Research (grant nos. 99-03-33248 and 01-03-32821) and the Leading Scientific Schools Program (grant no. 00-15-97429).

REFERENCES

1. *Singlet O_2*, Frimer, A.A., Ed., Boca Raton: CRC, 1985, vols. I–IV.
2. Krasnovskii, A.M., Jr., *Sovremennye problemy lazernoi tekhniki* (Modern Problems of Lazer Technics), Moscow: VINITI, 1990, vol. 3, p. 63.
3. Raad, O., *Z. Biol.*, 1900, vol. 39, p. 524.
4. Tappeiner, H. and Jodlbauer, A., *Muench. Med. Wochensch*, 1903, vol. 1, p. 2042.
5. *Lasers and Hematoporphyrin Derivative in Cancer*, Hayata, J. and Dougherty, T.J., Eds., New York: Igaku-Shoin, 1983.
6. Lissi, E.A., Encias, M.V., Lemp, E., and Rubio, M.A., *Chem. Rev.*, 1993, vol. 93, p. 699.
7. Clennan, E.L., *Acc. Chem. Res.*, 2001, vol. 34, no. 11, p. 875.
8. Rougee, M., Bensasson, R.V., Land, E.J., and Pariente, R., *Photochem. Photobiol.*, 1988, vol. 47, p. 485.
9. Ivanov, V.B., Shlyapintokh, V.Ya., Khvostach, O.M., Shapiro, A.B., and Rozanysev, E.G., *J. Photochem.*, 1975, vol. 4, p. 313.
10. Darmanyan, A.P., Foote, C.S., and Jardon, P.J., *J. Phys. Chem.*, 1995, vol. 99, no. 31, p. 11854.
11. Darmanyan, A.P., Gregory, D.D., Guo, Y., Jenks, W.S., Burel, L., Eloy, D., and Jardon, P., *J. Am. Chem. Soc.*, 1998, vol. 120, no. 2, p. 396.
12. Guiraud, H.J. and Foote, C.S., *J. Am. Chem. Soc.*, 1976, vol. 98, no. 7, p. 1984.
13. Darmanyan, A.P. and Tatikolov, A.S., *J. Photochem.*, 1986, vol. 32, no. 2, p. 157.
14. Gekhman, A.E., Moiseeva, N.I., Minin, V.V., Larin, G.M., and Moiseev, I.I., *Mendeleev Commun.*, 1997, p. 221.
15. Gekhman, A.E., Moiseeva, N.I., Minin, V.V., Larin, G.M., and Moiseev, I.I., *Inorg. Chem.*, 1999, vol. 38, p. 3444.
16. Moiseeva, N.I., Gekhman, A.E., Minin, V.V., Larin, G.M., Bashtanov, M.E., Krasnovskii, A.A., and Moiseev, I.I., *Kinet. Katal.*, 2000, vol. 41, no. 2, p. 191.
17. Gekhman, A.E., Moiseeva, N.I., Timokhina, E.N., Bozhenko, K.V., Minin, V.V., Larin, G.E., Bashtanov, M.E., Krasnovskii, A.A., and Moiseev, I.I., *Zh. Fiz. Khim.*, 2000, vol. 74, no. 3, p. 435.
18. Kovalev, Yu.V., Moiseeva, N.I., Minin, V.V., Larin, G.M., Krasnovskii, A.A., Gekhman, A.E., and Moiseev, I.I., *Dokl. Akad. Nauk*, 2002, vol. 381, no. 1, p. 74.
19. Shol'ts, K.F. and Ostrovskii, D.N., *Metody sovremennoi biokhimii* (Methods of Modern Biochemistry), Moscow: Nauka, 1975, p. 52.
20. Larin, G.M., Zvereva, G.A., Minin, V.V., and Rakitin, Yu.V., *Zh. Neorg. Khim.*, 1988, vol. 33, no. 8, p. 2011.
21. Egorov, S.Yu. and Krasnovsky, A.A., Jr., *SPIE Proc.*, 1990, vol. 1403, p. 611.
22. Krasnovsky, A.A., Jr., *Photochem. Photobiol.*, 1979, vol. 29, no. 1, p. 29.
23. Egorov, S.Yu., Kamalov, V.F., Koroteev, N.I., Krasnovsky, A.A., Jr., Toleutaev, B.N., and Zinukov, S.V., *Chem. Phys. Lett.*, 1989, vol. 163, no. 5, p. 421.
24. Krasnovskii, A.A., Jr., *Sovremennye problemy lazernoi fiziki* (Modern Problems of Laser Physics), Moscow: VINITI, 1990, vol. 3.
25. Niu, J.Q. and Mendenhall, G.D., *J. Am. Chem. Soc.*, 1992, vol. 114, p. 165.
26. Khan, A.U. and Kasha, M., *J. Chem. Phys.*, 1963, vol. 39, no. 8, p. 2105.
27. Kanofsky, J.R., Sugimoto, H., and Sawyer, D.T., *J. Am. Chem. Soc.*, 1988, vol. 110, p. 3698.
28. Hamann, H.J., Dahlmann, J., and Huft, E., *Oxid. Commun.*, 1980, vol. 1, p. 183.
29. Aubry, J.M., *J. Am. Chem. Soc.*, 1985, vol. 107, p. 5844.
30. Böhme, K. and Brauer, H.-D., *Inorg. Chem.*, 1992, vol. 31, no. 16, p. 3468.
31. Samuni, A. and Czapski, G., *Isr. J. Chem*, 1969, vol. 91, p. 4673.
32. Setaka, M., Kirino, Y., Ozawa, T., and Kwan, T., *J. Catal.*, 1969, vol. 15, p. 209.
33. Berdnikov, V.M. and Schastnev, P.V., *Kinet. Katal.*, 1975, vol. 16, no. 1, p. 83.
34. Molin, Yu.N. and Ermolaev, V.K., *Kinet. Katal.*, 1961, vol. 2, no. 3, p. 358.
35. *Handbook of Chemistry and Physics*, Hodgman, C.D., Weast, R.C., and Selby, S.M., Eds., Cleveland: Chemical Rubber, 1955, vol. 2.

36. Aquilanti, V., Ascenzi, D., Bartolomei, M., Cappelletti, D., Cavali, S., de Castro Vitores, M., and Pirani, F., *J. Am. Chem. Soc.*, 1999, vol. 121, p. 10794.
37. Long, C.A. and Ewing, C.E., *J. Chem. Phys.*, 1973, vol. 58, no. 11, p. 4824.
38. Goodman, L. and Brus, L.E., *J. Chem. Phys.*, 1977, vol. 67, no. 10, p. 4398.
39. Brunetti, B., Liutti, G., Luzzatti, E., *et al.*, *J. Chem. Phys.*, 1981, vol. 74, no. 12, p. 6734.
40. Azyazov, V.N., Nikolaev, V.D., Svistun, M.I., and Ufimtsev, N.I., *Kvant. Elektron.*, vol. 28, no. 3, p. 212.
41. Ding, A., *Z. Phys. D.*, 1989, vol. 12, p. 253.
42. Cacace, F., de Petris, G., and Troiani, A., *Angew. Chem. Int. Ed. Engl.*, 2001, vol. 40, p. 4062.
43. Lewis, G.N., *J. Am. Chem. Soc.*, 1924, vol. 46, p. 2027.
44. Pauling, L., *The Nature of the Chemical Bond*, Ithaca: Cornell Univ. Press, 1960.
45. Leckenby, R.E. and Robbins, E.J., *Proc. R. Soc.*, 1966, vol. 291, p. 389.
46. Leckenby, R.E., Robbins, E.J., and Trevalion, P.A., *Proc. R. Soc. A*, 1964, vol. 280, p. 409.
47. Ewing, G.E., *Angew. Chem.*, 1972, vol. 12, p. 570.
48. Eyring, H., Hirschfelder, I.O., and Taylor, H.S., *J. Chem. Phys.*, 1936, vol. 4, p. 479.
49. Orlando, J.J., Tyndall, G.S., Nickerson, K.E., and Calver, J.G., *Geophys. Res. Lett.*, 1991, vol. 96, p. 20755.
50. Gorelli, F.A., Ulivi, L., Santoro, M., and Bini, R., *Phys. Rev. Lett.*, 1999, vol. 83, no. 20, p. 4093.
51. Lipikhin, N.P., *Neorganicheskie perekisnye soedineniya* (Inorganic Peroxide Compounds), Vol'nova, I.I., Ed., Moscow: Nauka, 1975.
52. Mullet, L., *Comp. Rend.*, 1927, vol. 185, p. 352.
53. Groh, P. and Kirrmann, A., *Comp. Rend.*, 1942, vol. 215, p. 275.
54. Seliger, H.H., *J. Chem. Phys.*, 1964, vol. 40, no. 10, p. 3133.
55. Brown, R.J. and Ogryzlo, E.A., *Proc. Chem. Soc.*, 1970, p. 117.
56. Huestis, D.L., Black, G., Edelstein, S.A., and Sharpless, R.L., *J. Chem. Phys.*, 1974, vol. 60, no. 11, p. 4471.
57. Matheson, I.B.C., Lee, Y., Yamanashi, B.S., and Wolbrast, M.L., *Chem. Phys. Lett.*, 1974, vol. 27, no. 3, p. 355.
58. Krasnovskii, A.A., Jr., *Biofizika*, 1976, vol. 21, no. 4, p. 748.
59. Krasnovskii, A.A., Jr. and Neverov, K.V., *Biofizika*, 1988, vol. 23, no. 5, p. 884.
60. Krasnovsky, A.A., Jr. and Neverov, K.V., *Chem. Phys. Lett.*, 1990, vol. 167, no. 6, p. 591.
61. Gekhman, A.E., Makarov, A.P., Nekipelov, V.M., Talzi, E.P., Polotnyuk, O.Ya., Zamaraev, K.I., and Moiseev, I.I., *Izv. Akad. Nauk SSSR, Ser. Khim.*, 1985, no. 7, p. 1686.
62. Moiseev, I.I., Shishkin, D.L., and Gekhman, A.E., *New. J. Chem.*, 1989, vol. 13, nos. 10–11, p. 683.
63. Gekhman, A.E., Moiseeva, N.I., and Moiseev, I.I., *Dokl. Akad. Nauk*, 1996, vol. 349, no. 1, p. 53.
64. Bozhenko, K.V., Timokhina, E.N., Gekhman, A.E., Moiseeva, N.I., and Moiseev, I.I., *Dokl. Akad. Nauk*, 2000, vol. 373, no. 3, p. 341.
65. Wright, J.S. and McKay, D.J., *Sci. Progr.*, 1999, vol. 82, no. 2, p. 151.